
Efficient Bayesian Updates for Deep Active Learning via Laplace Approximations

Denis Huseljc* Marek Herde Lukas Rauch Paul Hahn Zhixin Huang
Daniel Kottke Stephan Vogt Bernhard Sick

University of Kassel, Hesse, Germany
*dhuseljc@uni-kassel.de

Abstract

Deep active learning (AL) selects batches of instances for annotation to avoid retraining deep neural networks (DNNs) after each new label. Employing a naive top- b selection can result in a batch of redundant (similar) instances. To address this, various AL strategies employ clustering techniques that ensure diversity within a batch. We approach this issue by substituting the costly retraining with an efficient Bayesian update. Our proposed update represents a second-order optimization step using the Gaussian posterior from a last-layer Laplace approximation. Thereby, we achieve low computational complexity by computing the inverse Hessian in closed form. We demonstrate that in typical AL settings, our update closely approximates retraining while being considerably faster. Leveraging our update, we introduce a new framework for batch selection through sequential construction, updating the DNN after each label acquisition. Furthermore, we incorporate our update into a look-ahead selection strategy as a feasible upper baseline approximating optimal batch selection. Our results highlight the potential of efficient updates to advance deep AL research.

1 Introduction

Active Learning (AL) sequentially selects instances for annotation by human experts, aiming to maximize model performance while minimizing labeling efforts. When combined with deep neural networks (DNNs), AL typically selects instances in batches rather than one at a time. The reason for this is that retraining DNNs after each label acquisition is computationally expensive, and delay can lead to additional costs since annotators' time is valuable [21].

In a naive top- b batch selection, a batch of b instances with the highest scores is chosen based on an informativeness measure. However, when many similar instances are present, this approach can result in significant redundancy within the batch (similar instances have a similar score). Many selection strategies have been developed to replace this naive selection [16]. These strategies often employ clustering techniques to ensure diverse batches, ensuring that instances within a batch are dissimilar to one another [16]. While effective in reducing redundancy, clustering does not guarantee optimal selection due to its heuristic motivation.

Orthogonal to these strategies, we explore the concept of efficient “retraining” in deep AL. If retraining were computationally feasible, researchers could place greater emphasis on the development of theoretically sound informativeness measures instead of using heuristic clustering approaches to ensure diversity. Additionally, selection strategies that aim to maximize future performance—strategies that have been shown to be near-optimal in traditional AL [35]—could be made feasible with DNNs. Therefore, we examine the concept of updating DNNs through a single optimization step as a proxy for retraining and explore its potential to enhance the AL process.

To underscore the requirements of such an update, consider strategies designed to maximize future performance. Typically, these use a look-ahead to select instances that significantly change model predictions. Specifically, they examine how adding unlabeled instances to the labeled pool and retraining the model affects predictions [35]. However, with a large number of unlabeled instances and the costly retraining process of DNNs, this approach becomes infeasible in deep AL. Therefore, instead of retraining, a highly efficient update method is required. The only work to realize this with DNNs is by [40], which employ an ensemble of DNNs combined with Monte Carlo (MC) updates via Bayes’ theorem. Although this update makes a look-ahead feasible, it remains suboptimal for several reasons: (i) the update requires an ensemble of DNNs, making the actual retraining time and memory demands inefficient; (ii) the update does not accurately reflect the performance of full retraining; and (iii) the updating process becomes inefficient with an increasing number of ensemble members.

In this article, we propose an efficient update method for DNNs in the context of AL for classification. Specifically, we transform an arbitrary DNN into a Bayesian neural network (BNN) by employing a last-layer Laplace approximation (LA) [8]. While the closed-form expression of the posterior allows us to leverage second-order optimization techniques, we ensure low computational complexity by computing the required inverse Hessian analytically. Unlike the MC-based update used in [40], our approach does not require an ensemble of DNNs, making it easily applicable and both memory- and training-efficient [8]. Additionally, as we utilize a single DNN, we can leverage pretrained foundation models [31], which are an essential part of modern AL strategies [16, 15]. The resulting update is fast and closely matches the performance of full retraining. Extensive studies across different data modalities demonstrate that our updates outperform the typically employed MC-based ones [40] in terms of speed and performance. Furthermore, we examine the proposed update in two distinct AL scenarios:

1. **Enhancing Existing Strategies with Immediate Label Utilization:** We propose a simple framework to improve existing strategies by immediately making use of acquired labels through the proposed updates. Rather than selecting the top- b highest-scoring instances simultaneously, we iteratively select the highest-scoring instance b times *but* update the model between each selection. This simple strategy, which approximates single-instance AL during batch construction, performs surprisingly well, outperforming naive top- b selection as well as selection strategies that employ clustering.
2. **Optimal AL with Look-Ahead Selection:** We investigate the potential of our update with a look-ahead selection strategy in an optimal AL setting. Specifically, we approximate an optimal selection strategy that maximizes future performance. Instead of retraining, we ensure computational feasibility by employing our update. The resulting strategy outperforms all competitors, showcasing that currently employed selection strategies have much potential for improvement.

Summary of Contributions

Efficient DNN Update: We propose an efficient update method for DNNs that employs a Laplace approximation and second-order optimization techniques. We enable low computational complexity through closed-form computation of the inverse Hessian.

Comprehensive Evaluation: We perform an extensive evaluation across data modalities, demonstrating that our update outperforms MC-based updates in both speed and accuracy.

Immediate Label Utilization: We develop a simple framework that employs our update to immediately incorporate acquired labels, improving existing selection strategies by updating the model during batch construction.

Optimal AL with Look-Ahead: We study our update in an optimal AL setting, making a near-optimal selection strategy as an upper baseline computationally feasible.

2 Related Work

Pool-based deep AL strategies can be divided into three types. Uncertainty-based methods, such as margin sampling [3, 38] and BALD [13], assume that instances with high predictive uncertainty are most informative. When selecting batches, these strategies pick the top- b highest-scoring instances, leading to redundancy. In contrast, diversity-based approaches like Core-Set [37] aim to select a diverse batch of instances by considering the feature representations of labeled and unlabeled

data. In practice, *hybrid strategies*, a combination of both types, have been shown to work well. BatchBALD [19] extends BALD by reducing redundant information within a batch. Badge [1] selects instances with high gradient norms and ensures diversity by employing k -MEANS++ in the gradient space. Typiclust [16] replaces the notion of uncertainty with typicality and selects typical instances from clusters obtained through k -MEANS.

Look-ahead strategies [35] remain underexplored in deep AL. They aim to select instances expected to improve the model’s performance the most by retraining for all possible candidate instances. In non-deep settings, such approaches have been shown to achieve near-optimal selection [35] while offering convergence guarantees [46]. However, adapting these strategies to deep AL is challenging due to the computational cost of retraining. To the best of our knowledge, BEMPS [40] is the only strategy to implement a look-ahead mechanism in deep AL. They employ deep ensembles and MC-based updates via Bayes’ theorem (see Sec. 3). while this update is computationally efficient, we show that its performance falls short compared to full model retraining.

Continual learning [9] updates models by only using new data, retaining knowledge from the previous one. Related techniques [18, 34] use conventional first-order optimization methods, deriving regularization terms from an LA that penalizes large deviations from prior knowledge. Unlike our method, these approaches require training over multiple epochs for the regularization term to have an impact. Used as an update (i.e., single optimization step), these strategies simplify to a first-order gradient step. Additionally, they assume large amounts of new data per task (thousands of instances), whereas our update method is designed batch construction in AL, ranging from a single to hundreds of instances. For example, a typical benchmark is to extend a dataset with a task consisting of all instance-label pairs of a new class (ca. 5,000 in MNIST).

More closely related to our work is **online learning** [17], which aims to sequentially and efficiently update models from incoming data streams. Traditional approaches often focus on linear [47] or shallow [22] models with maximum-margin classification. However, applying online learning to DNNs remains difficult due to issues such as convergence, vanishing gradients, and large model sizes [36, 44]. Sahoo et al. [36] proposed a method that modifies a DNN’s architecture to facilitate updates. We argue that this is restrictive in state-of-the-art settings, given the increasing reliance on pretrained foundation models [10, 31]. Recently, [20] proposed Bayesian online inference, which is also used in [40]. This method samples hypotheses (e.g., via MC-Dropout) from a BNN’s posterior and weights them by the likelihood for new arriving data. However, the empirical results raise concerns about its feasibility in high-dimensional parameter spaces. We refer to these as MC-based updates.

BNNs [41] induce a prior distribution on parameters of a DNN and learn a posterior distribution given data. MC-Dropout [12] uses dropout to obtain a distribution over predictions. While it is simple to use, its inference is inefficient, and it provides suboptimal uncertainty estimates [32]. Deep ensembles [24] are known for their superior uncertainty estimates but are train and memory inefficient [32]. LAs [8] approximate the posterior as a Gaussian, with the MAP estimate as the mean and the inverse Hessian as the covariance. As computing this Hessian is expensive for large DNNs, LA is often used only in the last layer [8].

Finally, we consider related approaches focusing on the **efficiency of AL**. Prior work [6] shows that smaller more efficient proxy models can be used for AL selection with minimal performance loss. Building on this, [45] employed the last layer of a DNN as a proxy model in their benchmark. Other efforts to improve efficiency revolve around sub-sampling strategies with warm starts [7]. In contrast, rather than improving efficiency of the AL cycle, we update the DNN *while constructing the batch*, immediately incorporating label information that guides the construction process.

3 Fast Bayesian Updates for Deep Neural Networks

In this section, we first introduce the general concept of Bayesian updates together with the variant MC-based updates [20, 40]. Afterward, we propose our novel method focusing on an efficient update of the Gaussian posterior distribution via last-layer LAs. For an introduction to LA, we refer to [8].

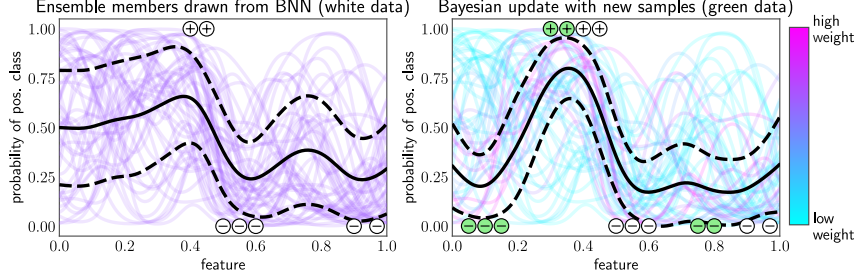


Figure 1: The left plot shows the predicted probabilities of the positive class for each hypothesis (colored lines) drawn from a BNN as well as the mean (black solid line) and standard deviation (black dashed line) of its predictive distribution. The right plot shows updated weights for each hypothesis and the predictive distribution after observing additional instances (green).

3.1 Bayesian Updates

We focus on classification problems with instance space \mathcal{X} and label space $\mathcal{Y} = \{0, \dots, K-1\}$. The primary goal in our setting is to efficiently incorporate the information of new instance-label pairs $\mathcal{D}^\oplus = \{(\mathbf{x}_n, y_n)\}_{n=1}^N \subset \mathcal{X} \times \mathcal{Y}$ into a DNN trained on dataset $\mathcal{D} \subset \mathcal{X} \times \mathcal{Y}$. Retraining the entire network on the extended dataset $\mathcal{D} \cup \mathcal{D}^\oplus$ results in high computational cost for a large dataset \mathcal{D} . Conversely, using the new data solely can cause catastrophic forgetting [34].

For this purpose, we employ BNNs with Bayesian updates as an efficient alternative to retraining. The main idea of BNNs is to estimate the posterior distribution $p(\boldsymbol{\omega}|\mathcal{D})$ over the parameters $\boldsymbol{\omega} \in \Omega$ given the observed training data \mathcal{D} using Bayes' theorem. The obtained posterior distribution over the parameters can then be used to specify the predictive distribution over a new instance's class membership via marginalization:

$$p(y|\mathbf{x}, \mathcal{D}) = \mathbb{E}_{p(\boldsymbol{\omega}|\mathcal{D})}[p(y|\mathbf{x}, \boldsymbol{\omega})] = \int p(y|\mathbf{x}, \boldsymbol{\omega})p(\boldsymbol{\omega}|\mathcal{D}) d\boldsymbol{\omega}. \quad (1)$$

Thereby, the likelihood $p(y|\mathbf{x}, \boldsymbol{\omega}) = [\text{softmax}(f^\omega(\mathbf{x}))]_y$ denotes the probabilistic output of a DNN with parameters $\boldsymbol{\omega}$, where $f^\omega : \mathcal{X} \rightarrow \mathbb{R}^K$ is a function outputting class-wise logits.¹

The formulation in Eq. (1) provides a theoretically sound way to obtain updated predictions. In particular, this is because the probabilistic outputs $p(y|\mathbf{x}, \boldsymbol{\omega})$ do not directly depend on the training data \mathcal{D} . Consequently, to obtain an updated predictive distribution, we do not need to update the parameters $\boldsymbol{\omega}$ directly but only the posterior distribution $p(\boldsymbol{\omega}|\mathcal{D})$. The updated posterior distribution $p(\boldsymbol{\omega}|\mathcal{D}, \mathcal{D}^\oplus)$ is found through Bayes' theorem, where the current posterior distribution $p(\boldsymbol{\omega}|\mathcal{D})$ is considered the prior and multiplied with the likelihood $p(y|\mathbf{x}, \boldsymbol{\omega})$ per instance-label pair $(\mathbf{x}, y) \in \mathcal{D}^\oplus$. As instances in \mathcal{D} and \mathcal{D}^\oplus are assumed to be independently distributed, we can simplify the likelihood and reformulate the parameter distribution as follows²:

$$p(\boldsymbol{\omega}|\mathcal{D}^\oplus, \mathcal{D}) \propto p(\boldsymbol{\omega}|\mathcal{D})p(\mathcal{D}^\oplus|\mathcal{D}, \boldsymbol{\omega}) \stackrel{\text{i.i.d.}}{=} p(\boldsymbol{\omega}|\mathcal{D})p(\mathcal{D}^\oplus|\boldsymbol{\omega}) = p(\boldsymbol{\omega}|\mathcal{D}) \prod_{(\mathbf{x}, y) \in \mathcal{D}^\oplus} p(y|\mathbf{x}, \boldsymbol{\omega}). \quad (2)$$

We refer to Eq. (2) as the *Bayesian update*.

The most common realization [20, 40] of this update is through MC-based BNNs, such as MC-Dropout and deep ensembles. These BNNs rely on samples (or hypotheses) $\boldsymbol{\omega}_1, \dots, \boldsymbol{\omega}_M$ drawn from an approximate posterior $q(\boldsymbol{\omega}|\mathcal{D})$. Research [40, 20] assumes that all hypotheses are equally likely to explain the observed data and have the same probability before updating. By updating the posterior distribution through Eq. (2), they weigh more likely hypotheses given the new data higher. We refer to these as MC-based updates with a formal definition given in Appendix A. Figure 1 illustrates this concept where different hypotheses $\boldsymbol{\omega}_1, \dots, \boldsymbol{\omega}_M \sim q(\boldsymbol{\omega}|\mathcal{D})$ are shown. Each hypothesis represents a possible true solution for the learning task (white instances). When new data (green instances) arrives, we weigh each hypothesis by its likelihood of explaining the new data and obtain an updated prediction without retraining. This results in an updated predictive distribution, as seen in bold in Fig. 1 (right).

¹We denote the i -th element of a vector \mathbf{b} as $[\mathbf{b}]_i = b_i$.

²We denote $p(y_1, \dots, y_N | \mathbf{x}_1, \dots, \mathbf{x}_N, \boldsymbol{\omega})$ with $\mathcal{D} = \{(\mathbf{x}_n, y_n)\}_{n=1}^N$ as $p(\mathcal{D}|\boldsymbol{\omega})$.

3.2 Fast Approximations of Bayesian Updates for Deep Neural Networks

Our update method is based on a combination of two concepts. First, instead of MC-based BNNs, we suggest using LAs on the last layer of a DNN. Second, we directly modify the approximate posterior distribution of the LA, providing a much more flexible way to adapt it to new data than reweighting. In the following, we explain each component in detail. For now, we focus on binary classification with $K = 2$, and refer to Appendix C for an extension to multi-class classification.

Last-layer LA: LAs approximate the (intractable) posterior distribution $p(\boldsymbol{\omega}|\mathcal{D})$ with a Gaussian centered on the maximum a posteriori (MAP) estimate with a covariance equal to the negative Hessian of the log posterior [8]. We denote this approximate distribution as

$$q(\boldsymbol{\omega}|\mathcal{D}) = \mathcal{N}(\boldsymbol{\omega}|\hat{\boldsymbol{\mu}}, \hat{\boldsymbol{\Sigma}}) \propto q(\boldsymbol{\omega}) \prod_{(\mathbf{x}, y) \in \mathcal{D}} p(y|\mathbf{x}, \boldsymbol{\omega}), \quad (3)$$

where $q(\boldsymbol{\omega})$ is a Gaussian prior distribution. The MAP estimate $\hat{\boldsymbol{\mu}}$ results from training on \mathcal{D} with conventional gradient optimization techniques. The covariance matrix $\hat{\boldsymbol{\Sigma}}$ is the inverse Hessian of the negative log posterior evaluated at the MAP estimate $\hat{\boldsymbol{\mu}}$ given training data \mathcal{D} . We model the posterior distribution only on the last layer of a DNN to ensure fast inference.

The benefits of using a last-layer LA are manifold. Given access to $q(\boldsymbol{\omega}|\mathcal{D})$ through a Gaussian, we enable *more flexible updates* compared to MC-based ones, as we can directly modify the mean and covariance. In contrast, MC-based updates only change the approximate distribution by reweighting hypotheses, leading to a strong dependency on the samples $\boldsymbol{\omega}_1, \dots, \boldsymbol{\omega}_M$. Last-layer LAs can be *integrated seamlessly* into nearly all DNNs, including pretrained models, as only the covariance has to be computed to obtain $q(\boldsymbol{\omega}|\mathcal{D})$. This is particularly important in deep AL, where recent findings highlight self-supervised learning as a crucial factor in selecting informative instances [16, 15]. Finally, compared to deep ensembles and MC-Dropout, last-layer LAs introduce *minimal computational overhead*. While deep ensembles require longer training and MC-dropout impairs the inference time, LAs simply need to calculate a covariance matrix after training and allow fast inference through techniques such as mean-field approximation [28].

Second-Order Update: The second concept focuses on the update step of the Gaussian distribution. Observing new data, we follow the same approach as in Eq. (3), but with $q(\boldsymbol{\omega}|\mathcal{D})$ as our prior:

$$q(\boldsymbol{\omega}|\mathcal{D}, \mathcal{D}^\oplus) = \mathcal{N}(\boldsymbol{\omega}|\hat{\boldsymbol{\mu}}^{\text{upd}}, \hat{\boldsymbol{\Sigma}}^{\text{upd}}) \propto q(\boldsymbol{\omega}|\mathcal{D}) \prod_{(\mathbf{x}, y) \in \mathcal{D}^\oplus} p(y|\mathbf{x}, \boldsymbol{\omega}), \quad (4)$$

where $\hat{\boldsymbol{\mu}}^{\text{upd}}$ and $\hat{\boldsymbol{\Sigma}}^{\text{upd}}$ represent the updated mean and covariance, respectively. The resulting updated posterior $q(\boldsymbol{\omega}|\mathcal{D}, \mathcal{D}^\oplus)$ is non-Gaussian due to $p(y|\mathbf{x}, \boldsymbol{\omega})$ being a categorical likelihood. Consequently, the closed-form computation of the integral in Eq. (1) becomes intractable. The basic idea of our update is to approximate the new posterior $q(\boldsymbol{\omega}|\mathcal{D}, \mathcal{D}^\oplus)$ by first applying a second-order optimization step via Gauss-Newton and then estimating the new covariance at that point. Thus, the updated mean and covariance are given by:

$$\hat{\boldsymbol{\mu}}^{\text{upd}} = \hat{\boldsymbol{\mu}} - \gamma \mathbf{H}^{-1}(\hat{\boldsymbol{\mu}}, \hat{\boldsymbol{\Sigma}}, \mathcal{D}^\oplus) \sum_{(\mathbf{x}, y) \in \mathcal{D}^\oplus} (p_x - y) \mathbf{h}_x, \quad (5)$$

$$\hat{\boldsymbol{\Sigma}}^{\text{upd}} = \mathbf{H}^{-1}(\hat{\boldsymbol{\mu}}^{\text{upd}}, \hat{\boldsymbol{\Sigma}}, \mathcal{D}^\oplus), \quad (6)$$

where \mathbf{h}_x denotes the representation of \mathbf{x} at the penultimate layer, $p_x = \text{sigmoid}(\mathbf{h}_x^\top \boldsymbol{\mu})$ is the probability for the positive class, and γ is a factor controlling the step size. The required updated Hessian can be computed efficiently in closed form following [39] by

$$\mathbf{H}^{-1}(\boldsymbol{\mu}, \boldsymbol{\Sigma}, \mathcal{A}) = \boldsymbol{\Sigma} - \sum_{(\mathbf{x}, y) \in \mathcal{A}} \frac{p_x(1-p_x)}{1 + \bar{\sigma}_x \cdot p_x(1-p_x)} (\boldsymbol{\Sigma} \mathbf{h}_x) (\boldsymbol{\Sigma} \mathbf{h}_x)^\top, \quad (7)$$

where $\bar{\sigma}_x = \mathbf{h}_x^\top \boldsymbol{\Sigma} \mathbf{h}_x$ is the predictive variance. The derivation can be found in Appendix D.

The idea behind using second-order optimization techniques is that they are more robust than first-order gradient optimization techniques due to the incorporation of curvature information of the log posterior. This results in a more accurate representation of the loss landscape, enabling more efficient

and robust parameter updates that are less sensitive to hyperparameter choices. A critical aspect of our method’s efficiency is that we do not need to recompute the Hessian from scratch. Instead, our updates leverage the covariance available through LAs and use the Woodbury identity [43] for closed-form inversion, significantly reducing computational overhead. Further, a common problem with last-layer LAs is that the Hessian can become a bottleneck when dealing with a large number of classes. To address this, we can approximate the Hessian in Eq. (7) by considering a Gaussian likelihood instead of a multi-class one, as also done in [26]. Lastly, we want to highlight that an assumption of an LA is that we are at the mode of a distribution, and adding more data violates this assumption. As we focus on AL and only update with a few (up to hundreds) instances at a time, this issue is less severe.

4 Bayesian Updating Experiments

In this section, we evaluate the efficiency of the proposed update by comparing it against competitors on various benchmark datasets for image and text classification. Our code is publicly available at <https://github.com/dhuseljic/dal-toolbox>.

4.1 Experimental Setup

Our **experimental design** is based on the work of [20]. First, we train a DNN on the training dataset \mathcal{D} (baseline). We then use this baseline DNN to evaluate a last-layer LA and related Bayesian updates on additional instance-label pairs \mathcal{D}^\oplus and compare these results to retraining the DNN on the complete dataset $\mathcal{D} \cup \mathcal{D}^\oplus$. We evaluate (i) the influence of the step size γ on chosen validation datasets, (ii) the impact of our update at different learning stages of the DNN, (iii) the impact of our update with increasing sizes of new arriving datasets, and (iv) the time efficiency of our update by considering the speed-up factor against retraining. For comparison, we consider MC-based updates by sampling 10k hypotheses from the approximate Gaussian posterior $q(\omega|\mathcal{D})$ and the less complex first-order updates only considering gradients. Note that the latter is equivalent to the continual learning strategy of [34], as we demonstrate in Appendix A. Since first-order updates do not use the Hessian, this comparison also allows us to assess the benefits of using second-order optimization. We exclude retraining solely on \mathcal{D}^\oplus , as we empirically found that it leads to catastrophic forgetting [18]. All performance metrics are averaged across 10 repetitions. For visual clarity, we do not report standard errors.

The datasets \mathcal{D} and \mathcal{D}^\oplus are randomly sampled from real-world datasets. We use three image and three text **benchmark datasets** commonly used in literature [16, 33] with varying complexity reflected through different numbers of classes. Table 1 gives an overview. A detailed summary for each dataset is provided in Appendix E.

Table 1: Overview of datasets.

Type	Dataset	# classes
Image	Cifar-10 [23]	10
	Snacks [29]	20
	DTD [5]	47
Text	DBPedia [2]	14
	Banking-77 [4]	77
	Clinic-150 [25]	150

The goal of an update method is to ensure both effectiveness and speed. To assess this, we use different **performance metrics**. To evaluate *effectiveness*, or how well an update or retraining generalizes, we measure accuracy. When experimenting with hyperparameters, accuracy is assessed on a 10% validation split. Otherwise, it is measured on the test dataset. An optimal update method should achieve the same performance as completely retraining the DNN with $\mathcal{D} \cup \mathcal{D}^\oplus$. To assess the *speed* of an update, we report the speed-up factor compared to retraining by dividing the time required for retraining by the time required for updating (Eqs. (6) and (7)). Retraining and updating times were recorded on an NVIDIA RTX 4090 GPU and an AMD Ryzen 9 7950X CPU, respectively.

We choose common pretrained DNN **architectures** from the literature [16, 15]. For image datasets, we employ a Vision Transformer (ViT) [11] with pretrained weights via self-supervised learning, complemented by a randomly initialized fully connected layer. Specifically, we use the DINOv2-ViT-S/14 model [31] with a feature dimension of $D = 384$ in its final hidden layer. For text datasets, we employ the transformer-based pretrained language model BERT [10]. We utilize BERT-BASED-UNCASED from the Huggingface library [42] with a feature dimension of $D = 768$ and a maximum sequence length of 512. We train each DNN by finetuning for 200 epochs, employing the Rectified Adam optimizer [27] with a training batch size of 64, a learning rate of 0.01 for images and 0.1 for text, and weight decay of 0.0001. In addition, we utilize a cosine annealing learning rate scheduler.

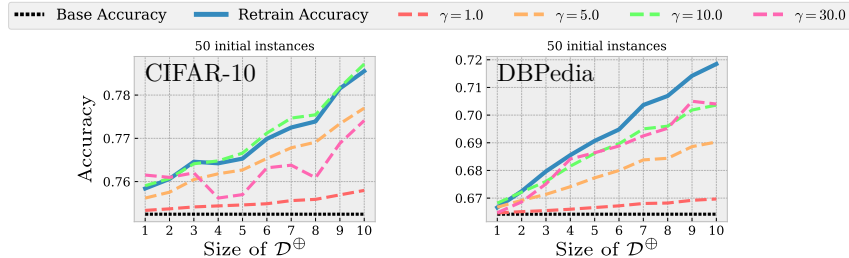


Figure 2: Accuracies after updating with different values for γ in comparison to the baseline DNN and retraining.

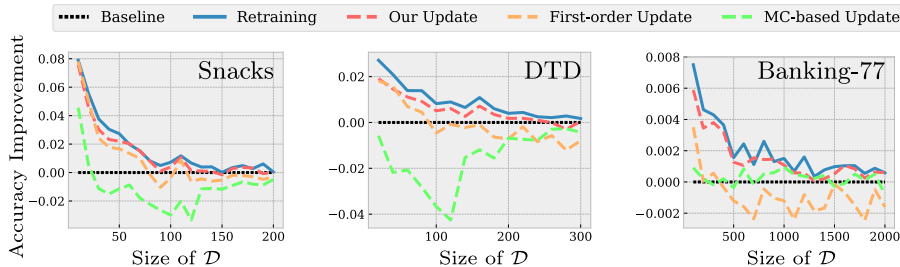


Figure 3: Accuracy improvement curves for benchmark datasets, showing the difference in accuracy between retrained and updated DNNs for varying sizes of \mathcal{D} .

These hyperparameters were determined empirically to be effective across all datasets by investigating the loss convergence on validation splits.

4.2 Experiments

Hyperparameter Ablation: In Eq. (6), we introduced the hyperparameter γ , which controls the step size of our update. Intuitively, this factor determines the extent to which the DNN is influenced by the new dataset \mathcal{D}^\oplus . This factor is essential to control the update process and avoid issues such as catastrophic forgetting. Similarly, first-order and MC-based updates also utilize this factor to mitigate such problems. For further details, we refer to Appendix A.

To investigate the influence of γ and determine a suitable value for all subsequent experiments, we conduct a simple ablation study on two datasets. The results of our update are shown here, while the results for first-order and MC-based updates can be found in Appendix B. We determine the value of γ in this manner since an extensive hyperparameter search for update methods is typically impractical in an online setting [9]. Hence, fixing a value beforehand is necessary. We randomly sample an initial dataset \mathcal{D} of 50 instances and train our baseline DNN. Subsequently, updates and retraining are performed on randomly sampled datasets $|\mathcal{D}^\oplus| \in \{1, \dots, 10\}$, and the accuracy is computed on a validation split. We repeat this process for different values of γ .

The resulting curves in Fig. 2 indicate that our update with \mathcal{D}^\oplus consistently achieves better performance than the baseline DNN that is only trained on \mathcal{D} . For both CIFAR-10 and DBPedia, updating with $\gamma = 1$ does not yield accuracies close to retraining, suggesting that the update is too weak. By increasing γ , we observe accuracies much closer to complete retraining, with $\gamma = 10$ being sufficient for CIFAR-10 and DBPedia. For CIFAR-10, we also notice that a very high value, i.e., $\gamma = 30$, can lead to worse performance, likely due to catastrophic forgetting. To ensure effective updates across all datasets, we will be using $\gamma = 10$ in all subsequent experiments. While this may not be optimal for some datasets, it should ensure a consistently working update in all cases.

Different Learning Stages: To investigate how our update behaves at different stages of learning, we train the baseline DNN on varying sizes of initial datasets \mathcal{D} and update it with a new dataset of fixed size $|\mathcal{D}^\oplus| = 10$. To better visualize the differences, we report accuracy improvement of updated/retrained DNNs relative to the baseline in Fig. 3. The results demonstrate that our updates provide the highest accuracy improvements across all datasets, highlighting the effective and

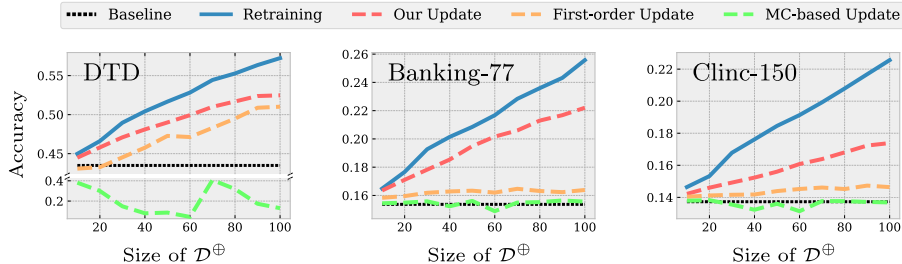


Figure 4: Accuracy curves for three benchmark datasets after updating and retraining DNNs for varying sizes of \mathcal{D}^\oplus .

consistent performance improvements of our update at different learning stages. While first-order and MC-based updates are also effective in earlier stages (when $|\mathcal{D}| < 50$), they tend to be less effective and even deteriorate accuracy in later stages. Compared to the first-order update, our update consistently enhances performance due to including the Hessian. As the Hessian considers curvature information about the posterior, the update is more robust regarding the choice of γ .

Varying Size of \mathcal{D}^\oplus : To investigate our update’s behavior with an increasing number of new data points in \mathcal{D}^\oplus , we train a baseline DNN with a fixed initial dataset $|\mathcal{D}| = 100$ and vary the size of the new dataset $|\mathcal{D}^\oplus| \in \{10, 20, \dots, 100\}$. We report the results for the most complex datasets DTD, Banking-77, and Clinc-150. In Fig. 4, we observe that as the size of \mathcal{D}^\oplus increases, the accuracy of retraining, our update, and the first-order update consistently improves. In contrast, MC-based updates result in worse accuracies than the baseline, indicating that it is not suited for an increasing size of \mathcal{D}^\oplus . Considering our update, we see that it consistently achieves better accuracies compared to competitors, regardless of the complexity of the dataset. Moreover, first-order updates seem to be less effective on the more complex datasets such as Banking-77 and Clinc-150, highlighting the importance of the Hessian.

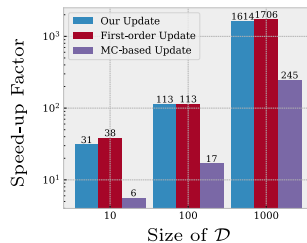


Figure 5: Speed-up of updates compared to retraining.

Time Comparison: Finally, to evaluate the speed of updates, we fix the size of the new dataset to $|\mathcal{D}^\oplus| = 10$ and compute the speed-up relative to retraining by varying the initial dataset size $|\mathcal{D}|$. Figure 5 presents the speed-up factors on CIFAR-10. All update methods are faster than retraining, with the first-order update being the fastest. For example, with an initial dataset of $|\mathcal{D}| = 1000$, the first-order update is about 1700 times faster than retraining. Notably, our update provides a similar speed-up factor while yielding more effective updates by using the closed-form Hessian update. Compared to MC-based updates, both the first-order and our update are significantly faster.

5 Deep Active Learning

In this section, we examine the proposed update in AL. First, we introduce a new framework that uses our updates to exploit label information during batch construction. Essentially, this approach mimics single instance AL, in which the model is retrained after each label acquisition. Next, we employ our update to approximate an optimal look-ahead strategy. Instead of obtaining future performance of the DNN with expensive retraining, we realize this through our update. Here, we average metrics over 30 repetitions to account for reproducibility challenges in AL [30]. Labeling budgets and acquisition sizes differ based on the complexity of a dataset. A more detailed experimental setup and all learning curves, including ones that report absolute values, are available in Appendix F.

Improved Batch Selection via Updates: A naive and suboptimal way of using sequential selection strategies for batch selection is to use the top- b scoring instances [21]. Our idea is to overcome the necessity of batch strategies by using the proposed update with sequential strategies as a fast alternative to retraining. Thus, we iteratively select the highest-scoring instance b times and update the DNN between each selection. After acquiring b labels, we retrain the DNN similar to batch selection strategies. An algorithm can be found in Appendix F.

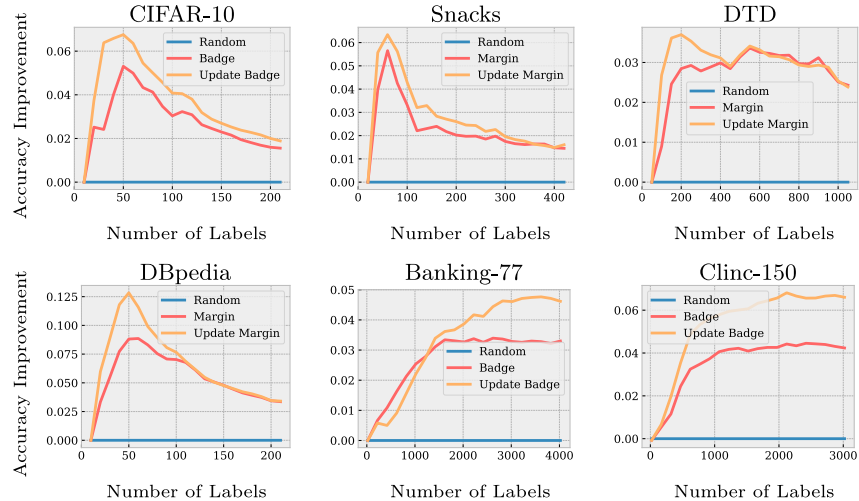


Figure 6: Accuracy improvement curves for different datasets showing the accuracy difference between the respective selection strategy and random instance selection.

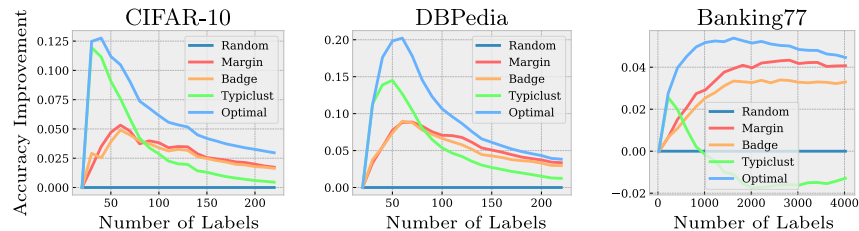


Figure 7: Accuracy improvement over random selection of popular selection strategies compared to our upper baseline approximating optimal batch selection.

The hypothesis is that already well-performing sequential selection strategies [38] can simply be used in a batch setting and that our framework can achieve higher performance compared to selecting the top- b instances. Here, we consider the widely used strategy Margin, which has proven to be effective in several studies [3]. Additionally, we are interested in whether this idea can also replace the diversity component of a batch selection strategy. Therefore, we also evaluate the popular strategy Badge [1] in combination with our updates.

Figure 6 shows the accuracy improvement curves relative to a random instance selection. The query strategies using our updates outperform the respective top- b selection strategies. Specifically, we see improved performance in early stages when redundancy within a batch plays an important role. Moreover, combining our update with Badge also results in improved accuracy. This indicates that *selecting a single instance and updating the DNN* leads to a more effective selection than using the k -MEANS++ algorithm as proposed in Badge.

Updating in Look-Ahead Strategies: The idea of look-ahead strategies is to select instances that, once labeled and added to the labeled pool, maximize the performance of the model [35]. Unlike uncertainty- or diversity-based approaches, look-ahead strategies select instances based on an optimal criterion: the model’s actual performance. However, they are often neglected in deep AL due to the high computational requirements. One of the biggest bottlenecks in the selection is retraining. DNNs are not well-suited for this due to their long training process. For this reason, we employ our proposed update to make this feasible.

Here, we consider a near-optimal strategy with access to ground truth information, including labels and validation datasets. It can be considered as an upper baseline in deep AL research. For the selection, we randomly sample 2000 subsets, each with a size equal to the acquisition size, and assess how their addition to the labeled pool affects the performance. The batch leading to the highest

performance gain is selected. While this approach would traditionally require 2000 times of retraining our update enables the efficient use of this strategy.

We also include the recently proposed Typiclust strategy, which demonstrated strong performance [16], especially in early stages of AL. Figure 7 presents the resulting accuracy improvement compared to random instance selection. Our optimal strategy, using updates rather than full retraining, performs exceptionally well, consistently outperforming all competitors. Based on these results, we can see that the current selection strategies still have much potential for improvement. Interestingly, we can see that Typiclust’s selection in the early stages of AL seems to be close to an optimal selection but declines in effectiveness in later stages.

6 Conclusion

We proposed an efficient second-order update for DNNs in AL using the Gaussian posterior of a last-layer LA. It achieves low computational complexity through a closed-form computation of the required inverse Hessian. An extensive experimental evaluation showed that the proposed update provides an efficient alternative to retraining. Based on this, we introduced a new batch selection framework by sequentially updating the DNN after each label, offering a new perspective on constructing batches without resorting to heuristics such as clustering. Additionally, we realized a look-ahead strategy as a feasible upper baseline approximating optimal batch selection, highlighting the great potential for improvement in current research on batch selection strategies. In future work, we plan to utilize the proposed updates to enhance look-ahead selection strategies [35] in deep AL. As these strategies are based on decision-theoretic principles, they naturally balance explorative and exploitative instance selection, a key challenge in AL.

References

- [1] Jordan T. Ash, Chicheng Zhang, Akshay Krishnamurthy, John Langford, and Alekh Agarwal. Deep Batch Active Learning by Diverse, Uncertain Gradient Lower Bounds. In *ICLR*, 2020.
- [2] Sören Auer, Christian Bizer, Georgi Kobilarov, Jens Lehmann, Richard Cyganiak, and Zachary Ives. Dbpedia: A nucleus for a web of open data. In *ISWC*, 2007.
- [3] Dara Bahri, Heinrich Jiang, Tal Schuster, and Afshin Rostamizadeh. Is margin all you need? an extensive empirical study of active learning on tabular data. *arXiv preprint arXiv:2210.03822*, 2022.
- [4] Iñigo Casanueva, Tadas Temčinas, Daniela Gerz, Matthew Henderson, and Ivan Vulić. Efficient intent detection with dual sentence encoders. In *NLP4ConvAI*, 2020.
- [5] M. Cimpoi, S. Maji, I. Kokkinos, S. Mohamed, , and A. Vedaldi. Describing textures in the wild. In *CVPR*, 2014.
- [6] Cody Coleman, Christopher Yeh, Stephen Mussmann, Baharan Mirzasoleiman, Peter Bailis, Percy Liang, Jure Leskovec, and Matei Zaharia. Selection via proxy: Efficient data selection for deep learning. In *ICLR*, 2020.
- [7] Arnav Mohanty Das, Gantavya Bhatt, Megh Manoj Bhalerao, Vianne R. Gao, Rui Yang, and Jeff Bilmes. Accelerating batch active learning using continual learning techniques. *TMLR*, 2023.
- [8] Erik Daxberger, Agustinus Kristiadi, Alexander Immer, Runa Eschenhagen, Matthias Bauer, and Philipp Hennig. Laplace redux-effortless Bayesian deep learning. In *NeurIPS*, 2021.
- [9] Matthias De Lange, Rahaf Aljundi, Marc Masana, Sarah Parisot, Xu Jia, Aleš Leonardis, Gregory Slabaugh, and Tinne Tuytelaars. A continual learning survey: Defying forgetting in classification tasks. *TPAMI*, 44(7):3366–3385, 2021.
- [10] Jacob Devlin, Ming-Wei Chang, Kenton Lee, and Kristina Toutanova. BERT: Pre-training of deep bidirectional transformers for language understanding. In *NAACL*, 2019.
- [11] Alexey Dosovitskiy, Lucas Beyer, Alexander Kolesnikov, Dirk Weissenborn, Xiaohua Zhai, Thomas Unterthiner, Mostafa Dehghani, Matthias Minderer, Georg Heigold, Sylvain Gelly, Jakob Uszkoreit, and Neil Houlsby. An image is worth 16x16 words: Transformers for image recognition at scale. In *ICLR*, 2021.

- [12] Yarin Gal and Zoubin Ghahramani. Dropout as a Bayesian approximation: Representing model uncertainty in deep learning. In *ICML*, 2016.
- [13] Yarin Gal, Riashat Islam, and Zoubin Ghahramani. Deep Bayesian active learning with image data. In *ICML*, 2017.
- [14] Jakob Gawlikowski, Cedric Rovile Njietcheu Tassi, Mohsin Ali, Jongseok Lee, Matthias Humt, Jianxiang Feng, Anna Kruspe, Rudolph Triebel, Peter Jung, Ribana Roscher, et al. A survey of uncertainty in deep neural networks. *Artificial Intelligence Review*, 56(1):1513–1589, 2023.
- [15] Sanket Rajan Gupte, Josiah Aklilu, Jeffrey J. Nirschl, and Serena Yeung-Levy. Revisiting Active Learning in the Era of Vision Foundation Models. *TMLR*, 2024.
- [16] Guy Hacohen, Avihu Dekel, and Daphna Weinshall. Active learning on a budget: Opposite strategies suit high and low budgets. In *ICML*, 2022.
- [17] Steven C H Hoi, Doyen Sahoo, Jing Lu, and Peilin Zhao. Online learning: A comprehensive survey. *Neurocomputing*, 459:249–289, 2021.
- [18] James Kirkpatrick, Razvan Pascanu, Neil Rabinowitz, Joel Veness, Guillaume Desjardins, Andrei A Rusu, Kieran Milan, John Quan, Tiago Ramalho, Agnieszka Grabska-Barwinska, Demis Hassabis, Claudia Clopath, Dharshan Kumaran, and Raia Hadsell. Overcoming catastrophic forgetting in neural networks. *PNAS*, 114(13):3521–3526, 2017.
- [19] Andreas Kirsch, Joost Van Amersfoort, and Yarin Gal. BatchBALD: Efficient and diverse batch acquisition for deep Bayesian active learning. In *NeurIPS*, 2019.
- [20] Andreas Kirsch, Jannik Kossen, and Yarin Gal. Marginal and Joint Cross-Entropies & Predictives for Online Bayesian Inference, Active Learning, and Active Sampling. *arXiv preprint arXiv:2205.08766*, 2022.
- [21] Andreas Kirsch, Sebastian Farquhar, Parmida Atighehchian, Andrew Jesson, Frédéric Branchaud-Charron, and Yarin Gal. Stochastic Batch Acquisition: A Simple Baseline for Deep Active Learning. *TMLR*, 2023.
- [22] Jyrki Kivinen, Alex Smola, and Robert C Williamson. Online learning with kernels. In *NeurIPS*, 2001.
- [23] Alex Krizhevsky. Learning multiple layers of features from tiny images. Master’s thesis, University of Toronto, 2009.
- [24] Balaji Lakshminarayanan, Alexander Pritzel, and Charles Blundell. Simple and scalable predictive uncertainty estimation using deep ensembles. In *NeurIPS*, 2017.
- [25] Stefan Larson, Anish Mahendran, Joseph J. Peper, Christopher Clarke, Andrew Lee, Parker Hill, Jonathan K. Kummerfeld, Kevin Leach, Michael A. Laurenzano, Lingjia Tang, and Jason Mars. An evaluation dataset for intent classification and out-of-scope prediction. In *EMNLP*, 2019.
- [26] Jeremiah Zhe Liu, Shreyas Padhy, Jie Ren, Zi Lin, Yeming Wen, Ghassen Jerfel, Zachary Nado, Jasper Snoek, Dustin Tran, and Balaji Lakshminarayanan. A simple approach to improve single-model deep uncertainty via distance-awareness. *JMLR*, 24(42):1–63, 2023.
- [27] Liyuan Liu, Haoming Jiang, Pengcheng He, Weizhu Chen, Xiaodong Liu, Jianfeng Gao, and Jiawei Han. On the variance of the adaptive learning rate and beyond. In *ICLR*, 2019.
- [28] Zhiyun Lu, Eugene Ie, and Fei Sha. Mean-field approximation to Gaussian-softmax integral with application to uncertainty estimation. *arXiv preprint arXiv:2006.07584*, 2020.
- [29] Matthijs. Snacks dataset. <https://huggingface.co/datasets/Matthijs/snacks>, 2021. Accessed: 2024-05-20.
- [30] Prateek Munjal, Nasir Hayat, Munawar Hayat, Jamshid Sourati, and Shadab Khan. Towards robust and reproducible active learning using neural networks. In *CVPR*, 2022.
- [31] Maxime Oquab, Timothée Darcet, Théo Moutakanni, Huy V Vo, Marc Szafraniec, Vasil Khalidov, Pierre Fernandez, Daniel Haziza, Francisco Massa, Alaaeldin El-Nouby, et al. DINOv2: Learning Robust Visual Features without Supervision. *TMLR*, 2023.
- [32] Yaniv Ovadia, Emily Fertig, Jie Ren, Zachary Nado, David Sculley, Sebastian Nowozin, Joshua Dillon, Balaji Lakshminarayanan, and Jasper Snoek. Can you trust your model’s uncertainty? Evaluating predictive uncertainty under dataset shift. In *NeurIPS*, 2019.

- [33] Lukas Rauch, Matthias Assenmacher, Denis Huseljic, Moritz Wirth, Bernhard Bischl, and Bernhard Sick. ActiveGLAE: A Benchmark for Deep Active Learning with Transformers. In *ECML*, 2023.
- [34] Hippolyt Ritter, Aleksandar Botev, and David Barber. Online structured Laplace approximations for overcoming catastrophic forgetting. In *NeurIPS*, 2018.
- [35] Nicholas Roy and Andrew McCallum. Toward Optimal Active Learning through Sampling Estimation of Error Reduction. In *ICML*, 2001.
- [36] Doyen Sahoo, Quang Pham, Jing Lu, and Steven CH Hoi. Online deep learning: learning deep neural networks on the fly. In *IJCAI*, 2018.
- [37] Ozan Sener and Silvio Savarese. Active learning for convolutional neural networks: A core-set approach. In *ICLR*, 2018.
- [38] Burr Settles. Active learning literature survey. Computer Sciences Technical Report 1648, University of Wisconsin–Madison, 2009.
- [39] David J Spiegelhalter and Steffen L Lauritzen. Sequential updating of conditional probabilities on directed graphical structures. *Networks*, 20(5):579–605, 1990.
- [40] Wei Tan, Lan Du, and Wray Buntine. Diversity enhanced active learning with strictly proper scoring rules. In *NeurIPS*, 2021.
- [41] Hao Wang and Dit-Yan Yeung. A survey on Bayesian deep learning. *CSUR*, 53(5):1–37, 2020.
- [42] Thomas Wolf, Lysandre Debut, Victor Sanh, Julien Chaumond, Clement Delangue, Anthony Moi, Pierric Cistac, Tim Rault, Remi Louf, Morgan Funtowicz, Joe Davison, Sam Shleifer, Patrick von Platen, Clara Ma, Yacine Jernite, Julien Plu, Canwen Xu, Teven Le Scao, Sylvain Gugger, Mariama Drame, Quentin Lhoest, and Alexander Rush. Transformers: State-of-the-art natural language processing. In *EMNLP*, 2020.
- [43] Max A Woodbury. *Inverting modified matrices*. Department of Statistics, Princeton University, 1950.
- [44] Jaehong Yoon, Eunho Yang, Jeongtae Lee, and Sung Ju Hwang. Lifelong learning with dynamically expandable networks. In *ICLR*, 2018.
- [45] Jifan Zhang, Yifang Chen, Gregory Canal, Arnav Mohanty Das, Gantavya Bhatt, Stephen Mussmann, Yinglun Zhu, Jeff Bilmes, Simon Shaolei Du, Kevin Jamieson, and Robert D Nowak. Labelbench: A comprehensive framework for benchmarking adaptive label-efficient learning. *DMLR*, 2024.
- [46] Guang Zhao, Edward Dougherty, Byung-Jun Yoon, Francis Alexander, and Xiaoning Qian. Uncertainty-aware active learning for optimal Bayesian classifier. In *ICLR*, 2021.
- [47] Martin Zinkevich. Online Convex Programming and Generalized Infinitesimal Gradient Ascent. In *ICML*, 2003.

A Related Bayesian Update Methods

We formally introduce Bayesian update methods used for comparison in the main part, including Monte Carlo (MC)-based updates and our method’s simpler variant, first-order updates.

A.1 MC-based Bayesian Updates

MC-based Bayesian neural networks (BNNs) such as deep ensembles and MC-Dropout draw samples, or hypotheses, from an (approximate) posterior distribution $q(\omega|\mathcal{D})$. To obtain these samples, deep ensembles train multiple randomly initialized deep neural networks (DNNs), while MC-Dropout randomly sets a portion of parameters to zero for multiple inference steps. We refer to [14] for an in-depth explanation of these techniques.

As MC-based BNNs only have access to these samples, the idea behind the MC-based update method is to weigh these samples. More specifically, MC-based updates, as used in [40], assume a priori that every hypothesis $\omega_1, \dots, \omega_M \sim q(\omega|\mathcal{D})$ is equally likely to explain the new dataset \mathcal{D}^\oplus . Hence, the approximate distribution *over the drawn members* can be defined as a categorical distribution³ with parameters $\hat{\mathbf{p}} = (\hat{p}_1, \dots, \hat{p}_M)^\top$:

$$q(\omega_m|\mathcal{D}) = \text{Cat}(m|\hat{\mathbf{p}}) = \hat{p}_m = 1/M, \quad (8)$$

where M is the number of drawn ensemble members. The updated posterior distribution, which includes the new dataset \mathcal{D}^\oplus , is computed through Bayes’ theorem:

$$q(\omega_m|\mathcal{D}^\oplus, \mathcal{D}) = \text{Cat}(m|\hat{\mathbf{p}}^{\text{upd}}) \propto q(\omega_m|\mathcal{D}) \prod_{(\mathbf{x}, y) \in \mathcal{D}^\oplus} p(y|\mathbf{x}, \omega_m) \quad (9)$$

$$= \hat{p}_m \prod_{(\mathbf{x}, y) \in \mathcal{D}^\oplus} [\text{softmax}(f^{\omega_m}(\mathbf{x}))]_y = \hat{z}_m, \quad (10)$$

which is a categorical distribution with parameters $\hat{\mathbf{p}}^{\text{upd}} = (\hat{p}_1^{\text{upd}}, \dots, \hat{p}_M^{\text{upd}})^\top$ that we obtain after normalizing $\hat{\mathbf{z}} = (\hat{z}_1, \dots, \hat{z}_M)^\top$. Intuitively, the importance of each hypothesis is determined by its likelihood of explaining the new dataset \mathcal{D}^\oplus . This approximation $q(\omega_m|\mathcal{D}^\oplus, \mathcal{D})$ of the posterior distribution allows us to make new predictions by evaluating the predictive distribution from Eq. (1) accordingly:

$$p(y|\mathbf{x}, \mathcal{D}^\oplus, \mathcal{D}) = \mathbb{E}_{q(\omega|\mathcal{D}^\oplus, \mathcal{D})}[p(y|\mathbf{x}, \omega)] \approx \sum_{m=1}^M p(y|\mathbf{x}, \omega_m) \cdot q(\omega_m|\mathcal{D}^\oplus, \mathcal{D}) \quad (11)$$

$$= \sum_{m=1}^M [\text{softmax}(f^{\omega_m}(\mathbf{x}))]_y \cdot \hat{p}_m^{\text{upd}}, \quad (12)$$

which is a weighted average of the sampled hypotheses. Employing the update from Eq. (10) may lead to catastrophic forgetting. Thus, to control the influence of the new dataset \mathcal{D}^\oplus , we introduce the hyperparameter γ :

$$q(\omega_m|\mathcal{D}^\oplus, \mathcal{D}) \propto \hat{p}_m \left(\prod_{(\mathbf{x}, y) \in \mathcal{D}^\oplus} [\text{softmax}(f^{\omega_m}(\mathbf{x}))]_y \right)^\gamma. \quad (13)$$

A.2 First-Order Bayesian Updates

Our proposed update method from the main text approximates the new posterior $q(\omega|\mathcal{D}, \mathcal{D}^\oplus)$ by applying an optimization step via Gauss-Newton and estimating the new covariance. For comparison, we evaluate an update based on a first-order optimization step, leading to a less complex and faster method. This also allows us to ablate the importance of the Hessian.

Assume a binary classification problem where we have an approximate posterior distribution $q(\omega|\mathcal{D}) = \mathcal{N}(\omega|\hat{\boldsymbol{\mu}}, \hat{\boldsymbol{\Sigma}})$ from an LA and observe the new dataset \mathcal{D}^\oplus . Our goal is to update the

³Equivalently, one can define the approximate distribution via multiple Dirac deltas.

approximate posterior distribution $q(\omega|\mathcal{D})$ by considering it as the new prior distribution:

$$q(\omega|\mathcal{D}, \mathcal{D}^\oplus) = \mathcal{N}(\omega|\hat{\mu}^{\text{upd}}, \hat{\Sigma}^{\text{upd}}) \propto q(\omega|\mathcal{D}) \prod_{(x,y) \in \mathcal{D}^\oplus} p(y|x, \omega). \quad (14)$$

The first-order update is defined by using a gradient optimization step to obtain an updated mean:

$$\hat{\mu}^{\text{upd}} = \hat{\mu} - \gamma \left(\sum_{(x,y) \in \mathcal{D}^\oplus} (\sigma(\mathbf{h}^T \hat{\mu}) - y) \mathbf{h}_x \right), \quad (15)$$

where γ is the step size (or learning rate) introduced to avoid catastrophic forgetting. The covariance matrix must only be recomputed at the update’s end if meaningful uncertainty estimates are of interest.

The updating strategy in Eq. (15) is equivalent to the continual learning strategy from [34]. There, the updated posterior distribution is defined as

$$\log p(\omega|\mathcal{D}, \mathcal{D}^\oplus) \propto \sum_{(x,y) \in \mathcal{D}^\oplus} \log p(y|x, \omega) - \frac{1}{2}(\omega - \hat{\mu})^T \hat{\Sigma}^{-1}(\omega - \hat{\mu}), \quad (16)$$

where the second term is the prior $q(\omega|\mathcal{D})$, penalizing large deviations of ω from the prior mean $\hat{\mu}$. The updated mean is then given by

$$\hat{\mu}^{\text{upd}} = \arg \max_{\omega} \sum_{(x,y) \in \mathcal{D}^\oplus} \log p(y|x, \omega) - \frac{1}{2}(\omega - \hat{\mu})^T \hat{\Sigma}^{-1}(\omega - \hat{\mu}). \quad (17)$$

[34] use multiple optimization steps via gradient descent to obtain the new mean $\hat{\mu}^{\text{upd}}$. Since we defined an update as a single optimization step and we start with $\omega = \hat{\mu}$, the regularization term evaluates to zero. Thus, the updated mean is obtained through a gradient step on the new data likelihood, simplifying the optimization to Eq. (15).

B Hyperparameter Ablation

For all introduced Bayesian update methods, the hyperparameter γ controls the influence of the new dataset \mathcal{D}^\oplus on the posterior distribution $q(\omega|\mathcal{D})$. In Sec. 4, we conducted a small ablation study, similar to a hyperparameter search, to determine an appropriate value for γ . We intentionally did not search a optimal value of γ for every dataset since extensive hyperparameter search for update methods is impractical in an online setting [9]. Using the same setup as in Sec. 4, we consider the CIFAR-10 and DBPedia datasets. Our baseline DNN is trained on a randomly sampled initial dataset \mathcal{D} of 50 instances. We then update and retrain the DNN with varying sizes of the new dataset $|\mathcal{D}^\oplus| \in \{1, \dots, 10\}$.

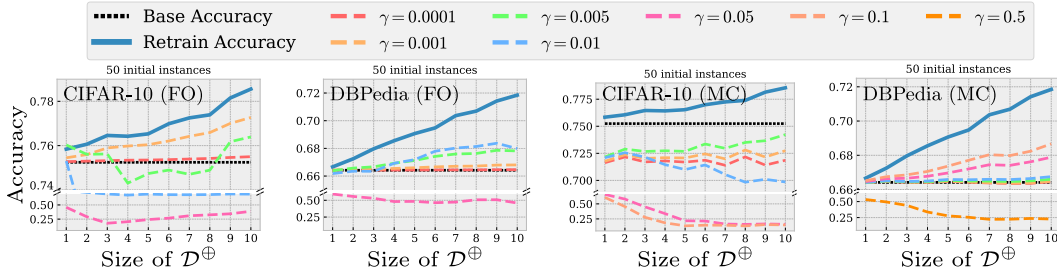


Figure 8: Accuracies after updating with different values for γ in comparison to the baseline DNN and retraining.

Considering the first-order update, we see that not all values of γ improve accuracy. Especially, high values can cause a collapse in accuracy, likely due to catastrophic forgetting. We find that updates with $\gamma = 0.001$ and $\gamma = 0.01$ perform best. Since $\gamma = 0.001$ generates the highest accuracy for CIFAR-10 and does not lead to a worse performance for DBPedia, we use it for the remaining experiments. Considering MC-based update, we see that no value of gamma provides an improvement in accuracy on CIFAR-10. In contrast, for DBPedia we see that $\gamma = 0.1$ improve accuracy the most. Considering the results across datasets, we select $\gamma = 0.005$ for images and $\gamma = 0.01$ for text.

C Multi-class Last-Layer Update

Here, we outline three different options for performing the update step for LA in a multi-class setting with $K > 2$. In a binary setting, a last-layer LA uses a parameter vector $\boldsymbol{\omega} \in \mathbb{R}^D$. However, in a multi-class setting, we have a parameter vector $\boldsymbol{\omega}_y$ for each class $y \in \mathcal{Y}$. In the literature, several approximations have been proposed to model these parameter vectors' distribution.

The most complex approximation would be to concatenate these vectors and model them through a multi-variate normal distribution:

$$q(\boldsymbol{\omega} | \mathcal{D}) = \mathcal{N}(\boldsymbol{\omega} | \hat{\boldsymbol{\mu}}, \hat{\boldsymbol{\Sigma}}) \text{ with } \boldsymbol{\omega}, \hat{\boldsymbol{\mu}} \in \mathbb{R}^{K \cdot D}, \hat{\boldsymbol{\Sigma}} \in \mathbb{R}^{(K \cdot D) \times (K \cdot D)}. \quad (18)$$

This approximation can estimate a covariance between each pair of parameters. However, this expressiveness comes at the cost of a large covariance matrix $\hat{\boldsymbol{\Sigma}}$ to be estimated. This is particularly costly for many classes K combined with a high feature dimension D from a DNN, such that corresponding updates via second-order optimization would no longer be efficient.

[39] presented a more efficient approximation in which the class-wise parameter vectors are arranged column-wisely as a matrix. Their joint distribution is then modeled through a matrix normal distribution:

$$q(\boldsymbol{\omega} | \mathcal{D}) = \mathcal{MN}(\boldsymbol{\omega} | \hat{\boldsymbol{\mu}}, \hat{\boldsymbol{\Gamma}}, \hat{\boldsymbol{\Sigma}}) \text{ with } \boldsymbol{\omega}, \hat{\boldsymbol{\mu}} \in \mathbb{R}^{D \times K}, \hat{\boldsymbol{\Sigma}} \in \mathbb{R}^{D \times D}, \hat{\boldsymbol{\Gamma}} \in \mathbb{R}^{K \times K}. \quad (19)$$

This approximation captures the covariance between each pair of parameter vectors via the matrix $\hat{\boldsymbol{\Gamma}}$ and each pair of hidden features via the matrix $\hat{\boldsymbol{\Sigma}}$. Both matrices have to be iteratively recomputed while updating. We refer to [39] for more details.

[26] presented an even faster approximation and showed its effectiveness in combination with an LA for supervised learning. Therefore, we employ this approximation in the multi-class setting. The idea is to determine an upper-bound covariance matrix shared by all class-wise parameter vectors in their respective multivariate normal distribution, which is then defined for class $y \in \mathcal{Y}$ as:

$$q(\boldsymbol{\omega}_y | \mathcal{D}) = \mathcal{N}(\hat{\boldsymbol{\mu}}_y | \hat{\boldsymbol{\Sigma}}) \text{ with } \boldsymbol{\omega}_y, \hat{\boldsymbol{\mu}}_y \in \mathbb{R}^D, \hat{\boldsymbol{\Sigma}} \in \mathbb{R}^{D \times D}. \quad (20)$$

The upper-bound covariance matrix $\hat{\boldsymbol{\Sigma}} \in \mathbb{R}^{D \times D}$ corresponds to the inverse Hessian of the negative log posterior evaluated at the MAP estimate $\hat{\boldsymbol{\mu}}$ given training data \mathcal{D} and a prior covariance matrix \mathbf{I} . It is given by

$$\hat{\boldsymbol{\Sigma}} = \mathbf{H}^{-1}, \text{ where } \mathbf{H} = \sum_{(\mathbf{x}, y) \in \mathcal{D}} p_{\mathbf{x}}^* (1 - p_{\mathbf{x}}^*) \mathbf{h}_{\mathbf{x}} \mathbf{h}_{\mathbf{x}}^T + \mathbf{I}, \quad (21)$$

where $p_{\mathbf{x}}^* = \max_y p(y | \mathbf{x}, \boldsymbol{\omega})$ is the maximum probability outputted by the the DNN. An even simpler approximation is to assume a Gaussian likelihood for the covariance, leading to the following formulation

$$\hat{\boldsymbol{\Sigma}} = \mathbf{H}^{-1}, \text{ where } \mathbf{H} = \sum_{(\mathbf{x}, y) \in \mathcal{D}} \mathbf{h}_{\mathbf{x}} \mathbf{h}_{\mathbf{x}}^T + \mathbf{I}. \quad (22)$$

which has been empirically shown to work more robustly when estimating uncertainties [26]. For this reason and its computational efficiency, we employ this approximation in our method.

Analog to the updates for binary classification in Eq. (6), we implement the updates of the mean parameter vector for class $y \in \mathcal{Y}$ and the covariance matrix $\hat{\boldsymbol{\Sigma}} \in \mathbb{R}^{D \times D}$ shared across the classes \mathcal{Y} given a new dataset \mathcal{D}^\oplus based on the Gauss-Newton algorithm leading to:

$$\hat{\boldsymbol{\mu}}_y^{\text{upd}} = \hat{\boldsymbol{\mu}} - \mathbf{H}^{-1}(\hat{\boldsymbol{\mu}}, \hat{\boldsymbol{\Sigma}}, \mathcal{D}^\oplus) \sum_{(\mathbf{x}, y') \in \mathcal{D}^\oplus} (p_{\mathbf{x}}^* - \delta(y = y')) \mathbf{h}_{\mathbf{x}}, \quad (23)$$

$$\hat{\boldsymbol{\Sigma}}^{\text{upd}} = \mathbf{H}^{-1}(\hat{\boldsymbol{\mu}}^{\text{upd}}, \hat{\boldsymbol{\Sigma}}, \mathcal{D}^\oplus), \quad (24)$$

where $\delta(\cdot)$ is the Dirac delta function. We efficiently compute the updated inverse Hessian using the Woodbury identity as presented in the upcoming Appendix D.

D Efficient Hessian Inversion via Woodbury Identity

Here, we provide the derivation of the update from Eq. (7), which uses the Woodbury (matrix) identity [43] for efficient inversion of the Hessian during updates. Assume we employed an LA and have the current approximate posterior distribution $q(\omega|\mathcal{D}) = \mathcal{N}(\omega|\hat{\boldsymbol{\mu}}, \hat{\boldsymbol{\Sigma}})$. To incorporate the information of the new dataset \mathcal{D}^\oplus into the LA’s current covariance $\hat{\boldsymbol{\Sigma}}$, we first need to calculate the Hessian of the new negative log posterior $q(\omega|\mathcal{D}, \mathcal{D}^\oplus)$ with respect to ω . The Hessian of the new negative log posterior $-q(\omega|\mathcal{D}, \mathcal{D}^\oplus)$ is given by

$$\mathbf{H} = -\nabla_{\omega}^2 \log q(\omega|\mathcal{D}, \mathcal{D}^\oplus) \quad (25)$$

$$= \mathbf{I} + \sum_{(\mathbf{x}, y) \in \mathcal{D}} p_x(1 - p_x) \mathbf{h}_x \mathbf{h}_x^T + \sum_{(\mathbf{x}, y) \in \mathcal{D}^\oplus} p_x(1 - p_x) \mathbf{h}_x \mathbf{h}_x^T, \quad (26)$$

$$= \hat{\boldsymbol{\Sigma}}^{-1} + \sum_{(\mathbf{x}, y) \in \mathcal{D}^\oplus} p_x(1 - p_x) \mathbf{h}_x \mathbf{h}_x^T, \quad (27)$$

where we see the updated Hessian is given by a sum of the old negative log posterior’s precision matrix with the precision matrix of the new dataset \mathcal{D}^\oplus . Note, however, that we require the *inverse* Hessian \mathbf{H}^{-1} for both the Gaussian posterior in the LA and the optimization step via Gauss-Newton. Depending on the size of \mathcal{D}^\oplus and the assumed likelihood for the Hessian, this computation can significantly slow down the efficiency of our update since we must compute an inverse with each new incoming batch of instances. Thus, to ensure efficient updates, we employ the Woodbury identity, which is given in a simplified form by

$$(\mathbf{A} + \mathbf{u}\mathbf{v}^T)^{-1} = \mathbf{A}^{-1} - \frac{\mathbf{A}^{-1}\mathbf{u}\mathbf{v}^T\mathbf{A}^{-1}}{1 + \mathbf{v}^T\mathbf{A}^{-1}\mathbf{u}}, \quad (28)$$

and allows us to obtain an updated inverse Hessian directly, avoiding calculation of the inverse of the updated precision matrix. Setting $\mathbf{u} = p_x(1 - p_x)\mathbf{h}_x$ and $\mathbf{v} = \mathbf{h}_x$, we obtain:

$$\mathbf{H}^{-1} = \left(\hat{\boldsymbol{\Sigma}}^{-1} + p_x(1 - p_x)\mathbf{h}_x \mathbf{h}_x^T \right)^{-1} \quad (29)$$

$$= \hat{\boldsymbol{\Sigma}} - \frac{p_x(1 - p_x)}{1 + \mathbf{h}_x \hat{\boldsymbol{\Sigma}} \mathbf{h}_x} \hat{\boldsymbol{\Sigma}} \mathbf{h}_x \mathbf{h}_x \hat{\boldsymbol{\Sigma}}, \quad (30)$$

which is the update from Eq. (7). In the multi-class setting, we employ the covariance matrix of Eq. (22) by assuming a Gaussian likelihood leading to the following inverse Hessian:

$$\mathbf{H}^{-1} = \left(\hat{\boldsymbol{\Sigma}}^{-1} + \mathbf{h}_x \mathbf{h}_x^T \right)^{-1} = \hat{\boldsymbol{\Sigma}} - \frac{\hat{\boldsymbol{\Sigma}} \mathbf{h}_x \mathbf{h}_x \hat{\boldsymbol{\Sigma}}}{1 + \mathbf{h}_x \hat{\boldsymbol{\Sigma}} \mathbf{h}_x}, \quad (31)$$

where we set $\mathbf{u} = \mathbf{v} = \mathbf{h}_x$.

E Summary of Datasets

CIFAR [23] consists of 60,000 colored images with a low resolution of 32×32 . There is a predetermined split of 50,000 images as training instances and 10,000 images as test instances. One variant of this dataset, **CIFAR-10**, is a coarse-grained task with ten broad classes such as automobile, dog, airplane, and ship. The classes are mutually exclusive meaning there is no overlap between, e.g., automobiles and trucks. **Snacks** [29] contains images of 20 different classes of snack foods. The 6,745 available images are split into 3,840 images for training, 955 for validation, and 920 for testing. Each image is 256 pixels wide while its height varies from 256 to 873 pixels. **DTD** [5] is a texture-focused dataset that consists of 5,640 images divided into 47 different classes. There are 120 images for each class and image sizes range between 300×300 and 640×640 . There is a predetermined split into three equally sized datasets for training, validation, and testing. **DBPedia** [2] is a larger text dataset with a medium class cardinality of 14 different classes. There are 14 different ontology-based classes. It consists of 560,000 training instances and 5,000 test instances. **Banking-77** [4] comes with a more complex task of conversational language understanding alongside intent detection. The combination of its high-class cardinality and a small pool of just 10,000 instances makes this data set even more challenging. **Clinc-150** [25] includes queries that are out-of-scope, i.e., queries that do not fall into any of the system’s supported intents. It contains 150 in-scope intent classes, each with 100 train, 20 validation, and 30 test instances. Additionally, there are 100 train and validation out-of-scope instances, and 1,000 out-of-scope test instances.

F Active Learning: Updates for Batch Selection and Look-Ahead

Algorithm: The main idea from Sec. 5 is to transform any sequential selection strategy into a batch strategy by using the proposed update method as a fast alternative to retraining. Typically, when using a sequential selection strategy, the naive idea in a batch setting is to select the instances that resulted in the top- b highest scores, where the score is defined by the respective selection strategy. Our method can now update the DNN after each acquired label instead of selecting the top- b instances. Hence, we have a similar scenario as if we would perform single-instance acquisitions but avoid the retraining after each acquired label. After aggregating a batch of b instances, we retrain the DNN.

Algorithm 1 summarizes this idea. Given a standard AL setting with labeled data \mathcal{L} and unlabeled data \mathcal{U} , we first calculate the approximate posterior distribution $q(\omega|\mathcal{L})$ via LA. Subsequently, we iteratively select a new instance \mathbf{x} and acquire its label y based on a given selection strategy $\alpha(\cdot)$ and update the approximate posterior distribution $q(\omega|\{(\mathbf{x}, y)\}, \mathcal{L})$ according to Eq. (6). We repeat this procedure for b acquisitions.

Algorithm 1 Updating in AL

Require: Labeled data \mathcal{L} , unlabeled data \mathcal{U} , selection strategy α , acquisition size b , BNN $q(\omega|\mathcal{L})$

- 1: New acquisitions $\mathcal{D}^\oplus = \{\}$
- 2: **for** $i = 1, \dots, b$ **do**
- 3: Acquire next instance $\hat{\mathbf{x}} = \operatorname{argmax}_{\mathbf{x} \in \mathcal{U}} \alpha(\mathbf{x}, \mathcal{U}, q(\omega|\mathcal{D}^\oplus, \mathcal{L}))$
- 4: Obtain new label \hat{y} for instance $\hat{\mathbf{x}}$
- 5: Extend new acquisitions $\mathcal{D}^\oplus \leftarrow \mathcal{D}^\oplus \cup \{(\hat{\mathbf{x}}, \hat{y})\}$
- 6: Remove acquisition from $\mathcal{U} \leftarrow \mathcal{U} \setminus \hat{\mathbf{x}}$
- 7: Update posterior distribution $q(\omega|\mathcal{D}^\oplus, \mathcal{L})$
- 8: **end for**
- 9: **return** Batch of new acquisitions \mathcal{D}^\oplus

Experiments: For the AL experiments in Sec. 5, we follow the recent work of [16, 15]. We use all datasets (cf. Tab. 1) and initialize the labeled pool \mathcal{L} with b randomly sampled instances. In each AL cycle, we select b new instances for labeling and fix the number of AL cycles to 20, resulting in a total budget of $B = 20 \cdot b$. The size b is determined based on the dataset’s complexity, ensuring that learning curves from random instance selection converge. Each AL selection strategy selected from 1,000 randomly sampled instances from the unlabeled pool \mathcal{U} to speed up the selection process, except for Typiclust, where we increased the number to 10,000 to avoid errors of k -MEANS. We employ the same architecture and training hyperparameters as described in the experimental setup in Sec. 4.1.

Improved Batch Selection: For the sequential selection strategy Margin [3], we select batches of instances by following Algorithm 1 instead of the top- b selection. In the case of Badge [1], we replace the k -MEANS++ algorithm that is typically used. Consequently, we select the instance with the highest gradient norm. All accuracy improvement curves are shown in Fig. 9. Associated learning curves reporting the absolute accuracy are shown in Fig. 10.

Approximating Optimal Batch Selection: In Sec. 5, we employed our update to approximate an optimal look-ahead batch selection strategy. The selection works as follows: We begin with a randomly initialized labeled pool. During selection, we deliberately avoid clustering schemes to simplify batch selection into picking a single instance per cluster. We argue that this enforced diversity can lead to suboptimal selection, especially in the later stages of active learning, where exploitation is more critical. Instead, we randomly sampled 2,000 batches, each matching the acquisition size. These batches likely include both diverse and non-diverse sets, allowing for exploration in the beginning and potential exploitation in the end. Each batch is used to update the model with our proposed method as a proxy for retraining. We then evaluated the performance of each updated model on a validation set. Finally, we selected the batch that yielded the highest performance improvement. The remaining accuracy improvement curves and learning curves reporting absolute values are shown in Figs. 11 and 12, respectively.

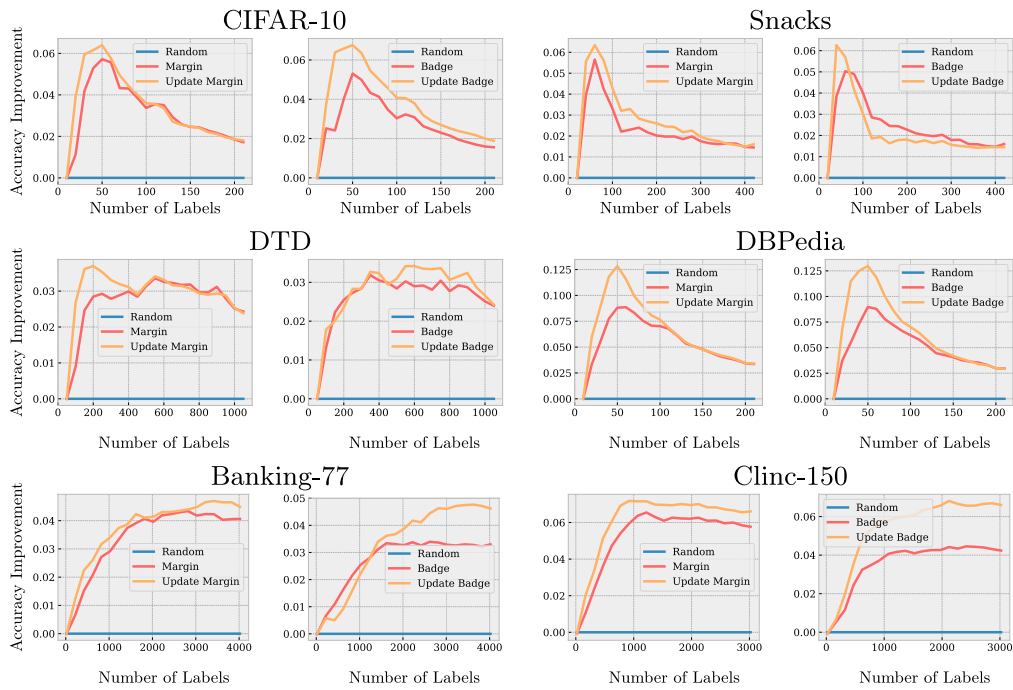


Figure 9: Accuracy improvement curves for different strategies and datasets showing the accuracy difference between the respective selection strategy and random instance selection.

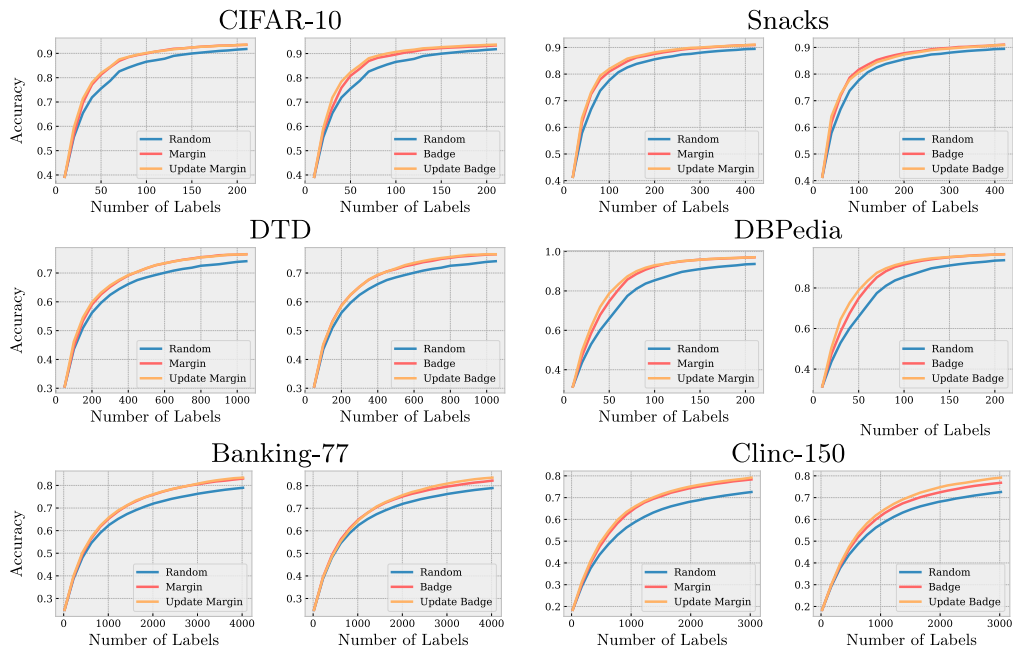


Figure 10: Learning curves for different strategies and datasets showing the accuracy.

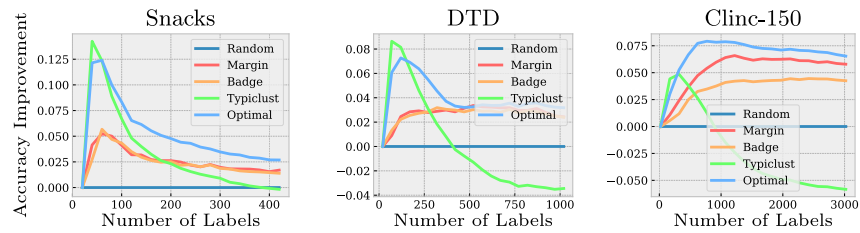


Figure 11: Accuracy improvement over random selection of popular selection strategies compared to our upper baseline approximating optimal batch selection.

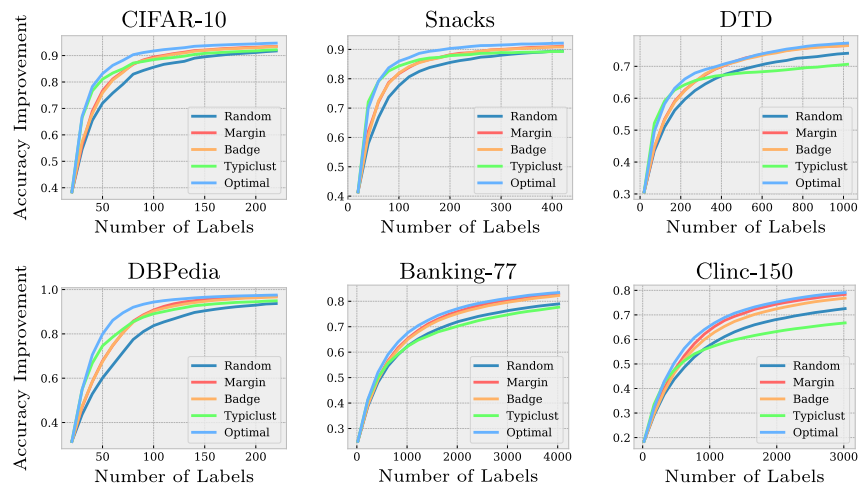


Figure 12: Learning curves reporting the accuracy of popular selection strategies compared to our upper baseline approximating optimal batch selection.